International Journal of Abrasive Technology

ISSN online: 1752-265X - ISSN print: 1752-2641
https://www.inderscience.com/ijat

Verification of deformation of thin mirror by polishing pressure using additive manufacturing

Daiya Yanagi, Shinya Morita

DOI: 10.1504/IJAT.2023.10054457

Article History:

Received:	15 June 2022
Last revised:	02 November 2022
Accepted:	13 January 2023
Published online:	12 May 2023

Verification of deformation of thin mirror by polishing pressure using additive manufacturing

Daiya Yanagi and Shinya Morita*

Graduate School of Engineering,
Tokyo Denki University,
5 Senju-asahi-cho, Adachi, Tokyo, 1208551, Japan
Email: 21kmf42@ms.dendai.ac.jp
Email: morita@mail.dendai.ac.jp
*Corresponding author

Abstract: In this study, magic and deformable mirrors were fabricated using an additive manufacturing (AM) process. This was to confirm the magic mirror effect caused by the grinding pressure of the mirrors produced by the AM-based manufacturing process. For verification, eight magic mirrors were fabricated under different conditions. The results showed that the magic mirror effect occurred on two mirrors with a diameter of 10 mm and wall thicknesses of 0.1 and 0.2 mm. AM is easy to machine thin-wall; therefore, a pneumatically deformable mirror was fabricated. The shape-control performance through air pressure fluctuations was confirmed. In this study, magic mirrors and deformable mirrors have been successfully fabricated using additive manufacturing technology. The method proposed in this study enabled the efficient production of lightweight and thin mirrors.

Keywords: additive manufacturing; magic mirror; magic mirror effect; deformable mirror; polishing pressure.

Reference to this paper should be made as follows: Yanagi, D. and Morita, S. (2023) 'Verification of deformation of thin mirror by polishing pressure using additive manufacturing', *Int. J. Abrasive Technology*, Vol. 11, No. 3, pp.233–246.

Biographical notes: Daiya Yanagi is currently a master course student at Tokyo Denki University. Since 2020, his research interests focus on additive manufacturing technology.

Shinya Morita received his PhD in Precision Engineering from the University of Tokyo, Japan in 2013. He was a research scientist in RIKEN, Japan before joining Tokyo Denki University as an associate professor in 2015. Since October 2016, he is a Professor at School of Engineering, Tokyo Denki University. He is an active member of The International Committee for Abrasive Technology (ICAT).

This paper is a revised and expanded version of a paper entitled 'Oriental magic mirror fabrication using additive manufacturing' presented at the 24th International Symposium on Advances in Abrasive Technology (ISAAT 2022), Guangzhou, China, 10 December 2022.

1 Introduction

In recent years, advances in science and technology have led to the development of next-generation devices, such as smart glasses and heads-up displays. As a result, there is a growing demand for lightweight, thin mirrors for use inside these. Thin mirrors have been studied in various fields, such as astronomical telescopes (Romeo et al., 2000; Ni et al., 2006; Cui et al., 2006; Miller et al., 1997), radiation (Spiga et al., 2016), and processing methods (Pilseong et al., 2017; Zhang et al., 2016). Traditionally, thin and lightweight mirrors have been manufactured by cutting or using moulds. However, there are issues, such as high cost and limitations to the structure of the mirror. Thin-walled structures have low rigidity, making machining difficult because of the vibrations generated during machining (Susanto et al., 2018; Umezu et al., 2019).

Additive manufacturing (AM) has attracted attention as a potential solution to these problems. AM technology is characterised by significant reductions in cost and lead time, as well as by allowing a high degree of freedom in design. Therefore, they are being actively studied in aerospace optics and other fields (Blakey-Milner et al., 2021). Selective laser melting (SLM) is a typical method used in three-dimensional (3D) metal printers. A mirror with a surface accuracy of 12.5 nm RMS, fabricated using SLM, has a 12.4 nm RMS after two years, indicating that it is stable over time (Hilpert et al., 2018). AM also makes it possible to manufacture lightweight mirrors and deformable mirrors with actuators inside the mirrors, which were previously impossible (Atkins et al., 2018; Roulet et al., 2020). Thus, AM enables the development of new ideas for metal mirrors.

The AM technology has made it possible to fabricate thinner mirrors. However, the residual stress from the heat of the laser and polishing pressure can cause unintended deformation. Although it is common practice to improve residual stress problems by heat treatment after fabrication, unintended deformation due to polishing pressure when fabricating thin mirrors remains unresolved. The unintended deformation of the thin-walled part creates the same effect as that of a magic mirror.

A magic mirror is a special mirror that has been handed down since ancient times in China and Japan (Saines et al., 1999). At first glance, this appears to be an ordinary mirror. However, when a mirror is illuminated with parallel rays of light, such as sunlight, and the reflected light shines on a white wall, a pattern engraved on the back of the mirror emerges. The mechanism is that the difference in mirror thickness creates a smooth concavo-convex shape of a few micrometres on the mirror surface, which causes the convergence and diffusion of reflected light (Figure 1) (Hibino, 1992). The concavo-convex shape of the backside of the reflective surface produces minute shape changes in the mirror surface; this effect, which affects the reflected light, is called the magic mirror effect (Furuki et al., 2014). Because magical mirror production is done manually by craftsmen, a shortage of craftsmen has become a problem in recent years (Yoneda et al., 1978). Therefore, a machining centre is used to fabricate magic mirrors, and is proposed as a method of digitising magic mirror creation skills (Furuki et al., 2014).

When thin mirror structures, such as mirrors for aerospace applications and deformable mirrors are fabricated by AM and polishing, there is a risk of the magic mirror effect occurring owing to the escape of material from thin-walled areas under pressure during polishing. In addition, the magic mirror effect leads to a reduction in optical performance. Therefore, it is necessary to predict the magic mirror effect in advance owing to differences in the thickness of thin-walled sections.

In this study, a magic mirror with a thin wall of less than 1 mm was fabricated using SLM, a metal AM technique, and the deformation caused by polishing pressure was verified. The detailed shape was observed using laser interferometry to investigate the amount of deformation. The usefulness of the Nagata patch was confirmed by simulating how reflected light was projected using the patch and comparing it with an actual projection image.

Figure 1 Mechanism of the magic mirror effect (see online version for colours)

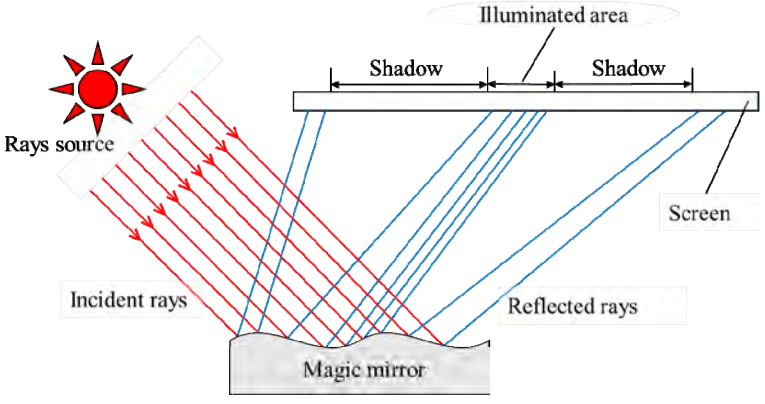

A new method using additive machining and polishing was adopted for this fabrication (Figure 2). The three-process method of AM, cutting, and polishing enables the creation of highly flexible shapes, including special shapes, using 3D complex structures, which can be fabricated at low cost. The possibility of fabricating a magic mirror by fabricating a thin mirror surface using the proposed method was focused on, and was fabricated and verified. The material used was SUS420J2 because it is often used as a material for metal mirrors and it can be used in metal 3D printers. Preliminary polishing tests confirmed that a mirror surface was obtained with Sa = 3.50 nm for the material after laminate moulding.

Figure 2 Manufacturing method (see online version for colours)

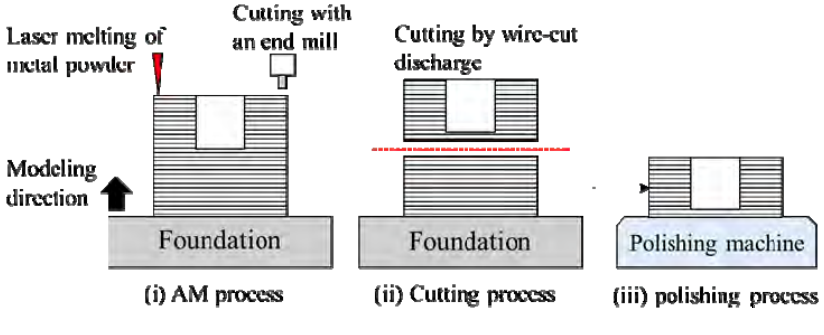

2 Mathematical approach for mirror design

The magic mirror effect is created by the deformation of thin-walled parts owing to the pressure during grinding. This is similar to the deflection concept in material mechanics.

First, we consider a one-dimensional structure such as a beam. When a beam of total length l [m] supported at both ends is subjected to an equally distributed load of ω [N], as shown in Figure 3, y_{max} is expressed as

$$y_{\max} = \frac{5}{384}\frac{\omega l^4}{EI_z} \tag{1}$$

where 'E' is Young's modulus of the material and 'I_z' is the area moment of inertia of the beam.

However, it is not easy for two-dimensional structures. Shapes such as circles and squares are relatively easy to predict, but complex shapes such as pictures are difficult to calculate. Therefore, to predict the magic mirror effect, the deformation simulation of the FEM analysis can be used for an efficient design.

Figure 3 Mechanical model of double-ended support beams (see online version for colours)

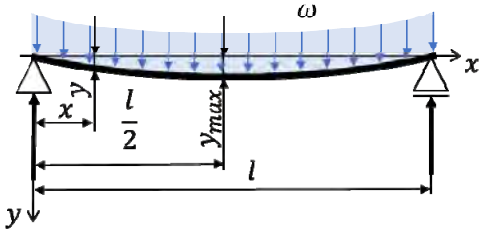

3 Magic mirror design and AM

The magic mirror was designed such that the projected image was T-shaped. Only the T-section was designed to be deformed by sculpting it to a thin thickness. Although more complex patterns can be realised using AM technology, this study attempted to fabricate a simple shape because observation of the magical mirror effect was the top priority (Figure 4). To observe the difference in deformation when the thickness is changed, six mirrors with the same diameter but different thicknesses of the letter part were produced. Two mirrors with different outer diameters and thicknesses were fabricated to observe the deformation caused by different diameters. To ensure that the amount of deformation was appropriate, the thickness was determined to be the same as that of a magic mirror with a character thickness of 0.1 mm using finite element analysis (Table 1).

Table 1 Scale of magic mirror

d	*T*	*t*	*s*	S_1	S_2
φ10	5	0.1, 0.2, 0.3, 0.4, 0.5, 1.0	3	7	7
φ50	15	0.5	15	36	35
φ100	15	1.0	30	72	70

The AM process used was an OPM250L (Sodick). The forming conditions were as follows: oxygen concentration of 3% or less, laser power of 400 W, laser speed of 700 mm/s, spot diameter of 0.2 mm. The inside of the lettering was stacked while cutting with end mills with diameters of 3.0, 1.5, and 1.0 mm to maintain shape accuracy. The thickness per layer was 0.05 mm. The next step was to cut unwanted sections using wire-cut electrical discharge machining.

4 Polishing process of magic mirror

During the polishing process, the magic mirror was polished using a plane lapping and polishing machine. After polishing with #800, #1,200, and #2,000 abrasive papers in reference to prior polishing tests, 0.1 μm colloidal alumina slurry was used. The basic polishing time is 60 s for each process. Table 2 summarises the polishing times of the magic mirror. Mirrors G and H were polished on a copper-grooved lapping surface plate because of their large diameters; a 9 μm diamond slurry was used.

Table 2 Polishing time of the magic mirror

Magic mirror name	*Thickness of lettering part t (mm)*	*Outer diameter d (mm)*	*Total polishing time for each polishing process (s)*			
			#800	*#1,200*	*#2,000*	*Colloidal alumina with double dilution of 0.1 μm particle size*
Mirror A	0.1	φ10	60	60	120	240
Mirror B	0.2	φ10	60	60	60	60
Mirror C	0.3	φ10	30	30	30	30
Mirror D	0.4	φ10	30	30	30	30
Mirror E	0.5	φ10	60	60	60	60
Mirror F	1.0	φ10	60	60	60	60
Mirror G	0.5	φ50	Used a copper grooved lapping surface plate and 9μm diamond slurry 600(s)			
Mirror H	1.0	φ100				

5 Production results

The polishing results for each mirror are presented in Table 3. The polishing amount was estimated from the focal length of the white interference microscope.

Mirror A had a non-uniform mirror surface when each polishing process was performed for 60 s. Therefore, the surface was polished with #2,000 for 60 s and colloidal alumina for an additional 120 s to obtain a uniform mirror surface. T-shaped deformations are visible on the completed mirror surface. The projected image was checked to confirm the magic-mirror effect. A T-shaped shadow was observed in the projected image (Figure 5).

3D shape measurements were performed to verify the detailed specular shape (Figure 6). Snap buckling was observed as a deformation caused by the grinding pressure. It was confirmed that there was deformation other than concave deformation when the thickness of the thin-walled part was insufficient.

Table 3 Polishing result

Mirror name	*Thickness of lettering part t (mm)*	*Magic mirror effect*	*Surface roughness*	*Amount of polishing (mm)*
Mirror A	0.1	Significant	-	-
Mirror B	0.2	Small	3.53 nm Sa	0.079
Mirror C	0.3	Not observed	7.50 nm Sa	-
Mirror D	0.4	Not observed	-	-
Mirror E	0.5	Not observed	4.55 nm Sa	0.108
Mirror F	1.0	Not observed	3.44 nm Sa	0.076
Mirror G	0.5	Not observed	Not mirror surface	-
Mirror H	1.0	Not observed	Not mirror surface	-

Note: '-' indicates unmeasured data.

Figure 5 Mirror A's (a) mirror surface after polishing and (b) projected image on the wall

(a) (b)

Figure 6 3D shape measurement of mirror A (see online version for colours)

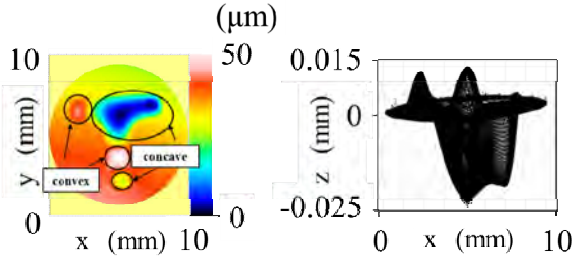

Mirror B produced a uniform mirror surface after polishing for 60 s each. Moreover, no T-shape deformation was visually confirmed. However, the observation of interference fringes by Newton's rings confirmed that the character areas were deformed convexly. The image projected onto the wall was T-shaped (Figure 7). The surface roughness after polishing is Sa = 3.53 nm. The polishing amount was measured from the change in the thickness of the workpiece before and after polishing and was found to be 0.079 mm (Figure 8).

Mirrors C and D were attempted by reducing the polishing time to 30 s for each process because it was thought that a sufficient optical surface could be obtained even if the polishing time was halved. Consequently, both specimens were uniformly polished, and no deformation was observed after polishing. The surface roughness after polishing

is Sa = 7.5 mm. In this design, the surface accuracy was sufficient even when the polishing time was halved (Figure 9).

Figure 7 Mirror B's (a) mirror surface after polishing and (b) projected image on the wall

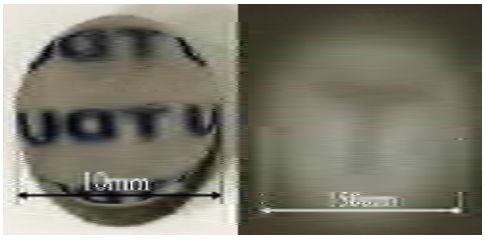

(a) (b)

Figure 8 Surface roughness of mirror B after polishing (see online version for colours)

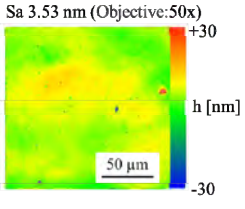

Figure 9 Result of polishing mirror C, (a) mirror surface (b) mirror surface observed by newton ring (c) surface roughness after polishing (see online version for colours)

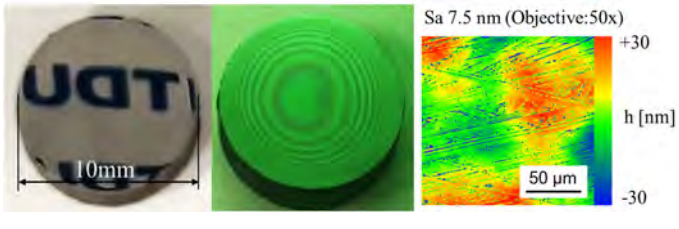

(a) (b) (c)

Figure 10 (a) Mirror surface of mirror E and (b) surface roughness after polishing (see online version for colours)

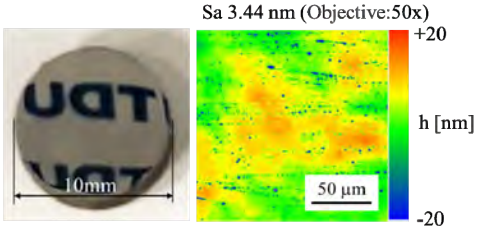

(a) (b)

Figure 11 (a) Mirror surface of mirror F and (b) surface roughness after polishing (see online version for colours)

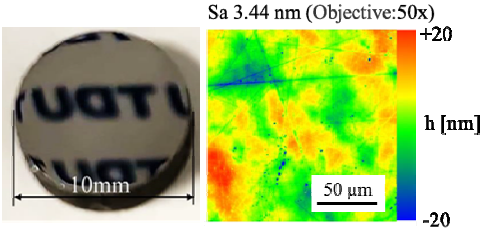

(a) (b)

Mirrors E and F were polished to estimate the polishing amount. Both mirrors were polished for 60 s for each process, and a uniform mirror surface was obtained. The surface roughness of mirror E is Sa = 4.55 nm, and the polishing amount is 0.108 mm (Figure 10). The surface roughness of mirror F was Sa = 3.44 nm, and the polishing amount was 0.076 mm (Figure 11).

Mirrors G and H were polished, and the polished surface was checked every 60 s. Mirror G showed no change after 7 min, becoming non-uniform only in the letter area. Finally, the polished surface was non-uniform despite 10 min of polishing. Similarly, for mirror H, no noticeable change was observed after 5 min. Even after 10 min of polishing, the polished surface was non-uniform (Figure 12). It was considered that the thickness was insufficient for the area of the thin-walled portion, which caused the material to escape and did not result in a uniform mirror surface. In addition, it is possible that the polishing was inadequate because a different abrasive was used than that for the other mirrors.

Figure 12 Polished surface (a) mirror G and (b) mirror H

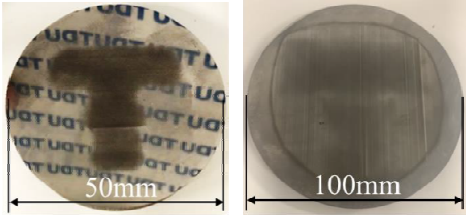

(a) (b)

6 Simulation of magic mirror surfaces by light ray tracking

For mirror A, which is a complex deformed structure, a projected image simulation was performed by ray tracing. The arrangement is such that parallel rays of light from the light source are reflected at a 45° angle and projected onto the screen. The distance L from the screen to the magic mirror surface was varied to check for changes in the projected image (Figure 13).

Figure 13 Arrangement of light in ray tracing simulation (see online version for colours)

Figure 14 Mirror A model using Nagata patch (see online version for colours)

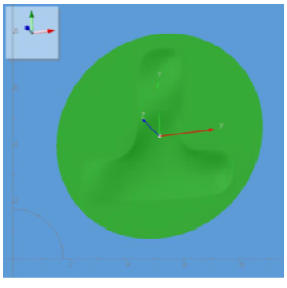

Figure 15 Prediction of the projected image of mirror A by ray tracing (see online version for colours)

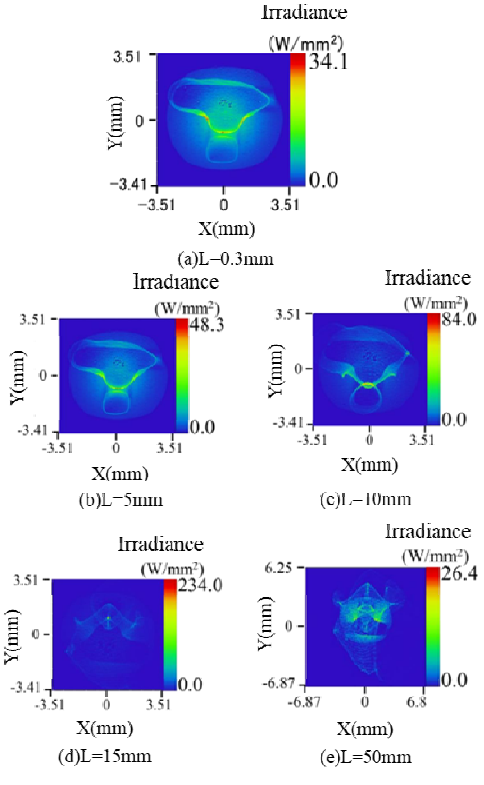

Based on the data obtained from the 3D shape measurements, simulations were performed using a model of mirror A created using the Nagata patch. The Nagata patch is a method of complementing a curved surface with a polygon mesh, which is useful for shape representation in ray tracing as it can accommodate local deformations. A model of mirror A with the Nagata patch is shown in Figure 14.

Consequently, a T-shape is visible in the projected image around L = 0.3 mm. Regarding the mixed shape of the unevenness, it was also observed that the unevenness varied, particularly in the lower part of the T-shaped vertical bar. When the value of L was further increased further, the image shape became less visible. This was because of the focal length of the mirror (Figure 15). It was confirmed that simulation by ray tracing is feasible for complex geometries and that deformation can be predicted from the magic mirror surface.

7 Manufacture of deformable mirror

Deformable mirrors are used in space telescopes, such as in adaptive optics, and are mostly deformed by piezoelectric or magnetostrictive elements (Zhu et al., 1999; Rousset et al., 2003). The proposed method could be used to realise shape deformation more simply; thus, pneumatic deformation was attempted. A closed space was created in the mirror, to which a tube was connected to the feed air and its shape was changed. The machining process and design procedures were the same as those for the magic mirrors. Owing to the air delivery mechanism, some geometries and dimensional values were adjusted (Figure 16). For the polishing process, the same conditions were used as for mirror G, which has the same dimensions. During the polishing process, additional polishing was performed as the polishing surface became non-uniform, for a total of one hour.

Figure 16 Design of deformable mirror (see online version for colours)

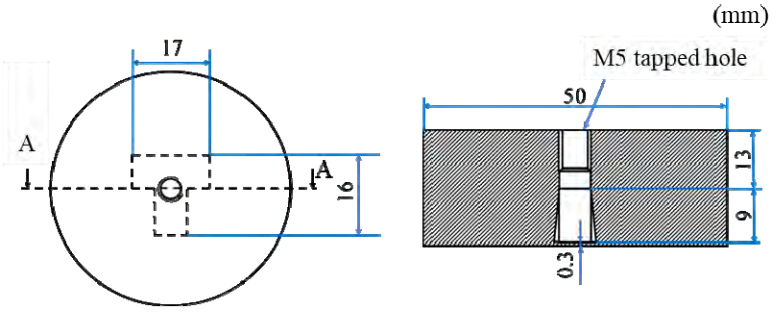

8 Results of deformable mirror manufacturing

The polishing results are shown in Figure 17. At the end of polishing, interference fringes were observed using a Newton ring, and it was found that a T-shaped convex deformation occurred even without pressurisation.

To examine the shape in more detail, a Fizeau laser interferometer was used to measure the shape (Figure 18). A T-shaped convex deformation was observed at the centre of the mirror surface, confirming an overall convex shape. Measurements showed that the deformation maximum was located almost at the centre of the y-axis, 24.48 mm, and that deformation of approximately 200 nm occurred.

Figure 17 Polished surface of (a) a deformed mirror and (b) observation by newton ring (see online version for colours)

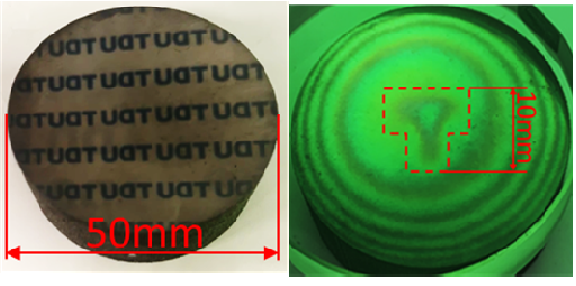

(a) (b)

Figure 18 Surface profile measurement results, (a) overall view (b) x-axis section (c) y-axis section (see online version for colours)

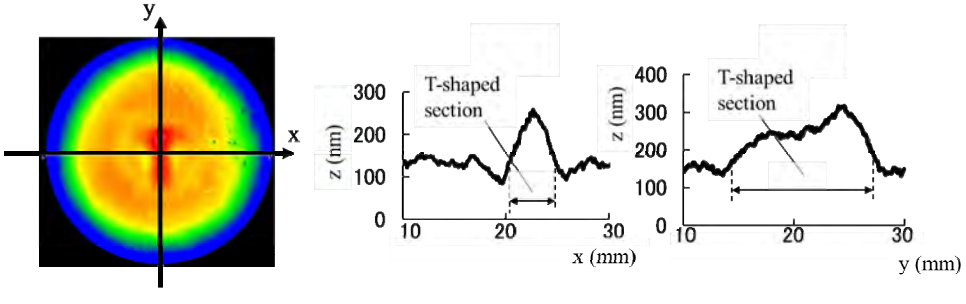

(a) (b) (c)

Figure 19 Confirmation of the magic mirror effect when deformable mirror air pressure is injected, (a) 0 MPa (b) 0.2 MPa

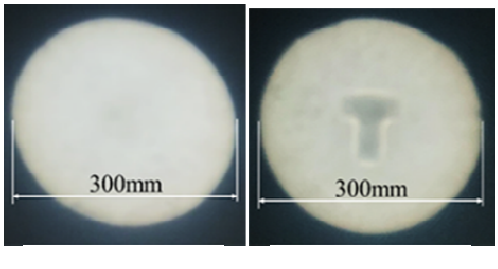

(a) (b)

Next, a deformation test was conducted using air pressure. The pressure inside the mirror was varied between 0~0.2 MPa and the projected image was checked, and the magic mirror effect was observed with deformation, as shown in Figure 19. Surface profiles were measured, and it was found that thin-walled areas could be deformed by air pressure (Figure 20). Observations were made at pressures from 0 to 0.2 MPa and the magnitude of deformation was confirmed by considering the maximum peak value at each pressure (Figure 21). The linear relationship between pressure and deformation and instantaneous deformation indicates that the pneumatic system can act as a deformable mirror.

Figure 20 Deformation shape at 0.2 MPa of applied pressure (see online version for colours)

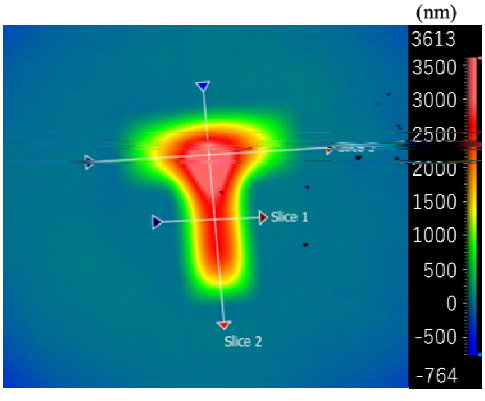

Figure 21 Deformation resulting from pressure

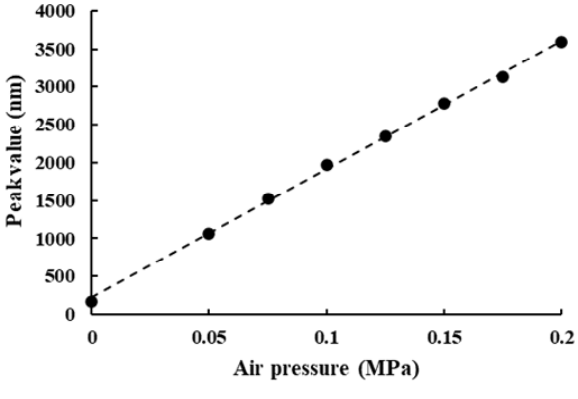

Note: Dashed line reveals a linear approximation of measured point.

9 Conclusions

In this study, through the manufacture of a magic mirror, the deformation of mirrors with a thin wall of less than 1 mm due to polishing pressure was observed using shape measurement.

Mirror A (0.1 mm) and B (0.2 mm) were observed to deform owing to the polishing pressure in the thin-walled areas. In addition, the magic mirror effect was successfully achieved. In addition, snap buckling was observed as a deformation shape for mirror A, indicating that the fabrication was as thin as possible. However, the deformation was unintentional; therefore, future work is required to control this deformation.

Mirrors C–F (0.3~1.0 mm) showed no deformation due to the polishing pressure. The lack of unintended deformation implies that the thin mirrors can be successfully manufactured.

Mirrors G (φ50) and H (φ100) cannot be uniformly polished on the character area. The deformation caused by the difference in diameter should be compared with that of the same abrasive.

The polishing amount was estimated based on the difference in the focal length of the white interferometer. The estimated values for the three mirrors were 0.076, 0.108, and 0.079 mm, respectively. However, this value is not accurate because of the paucity of data and the fact that it is an estimate based on focal length. In the future, improvements are needed, such as collecting more data and physically measuring them.

For mirror A, with a complex deformed shape, the projected image was predicted by a ray-tracing simulation using the Nagata patch. It was confirmed that ray-tracing simulation is possible even for complex shapes and that the deformation can be predicted from the magic mirror surface.

A deformable mirror was fabricated, and its shape was controlled by varying the air pressure. The linearity of the relationship between the deformation and pressure was confirmed.

In this study, the AM technology successfully produced magic mirrors and deformable mirrors. This time it was a simple shape; however, in the future more complex shapes will be realised using AM technology. If deformation due to grinding pressure can be performed in the intended shape, it can be applied to a variety of industrial products. This should be investigated for use in future thin film production.

Acknowledgements

We would like to thank Mr. Haruki Mochizuki of Tokyo Denki University for the preliminary study of the design and fabrication of the magic mirror, Mr. Tsubasa Takayama of Sodick Co., Ltd. for the metal 3D printer fabrication and wire EDM of the magic mirrors, Mr. Yutaro Koyama of YAMAWA MFG. Co., Ltd. for machining the female threads of the deformable mirror fabrication, Dr. Yutaka Yamagata of the RIKEN Center for Advanced Photonics for the mirror shape measurements by laser, and Shinya Kaneko of Graduate School of Engineering, Tokyo Denki University for the ray-tracing simulation.

References

Atkins, C. et al. (2018) ‘Topological design of lightweight additively manufactured mirrors for space’, *Proc. SPIE 10706, Advances in Optical and Mechanical Technologies for Telescopes and Instrumentation III*, p.107060I .

Blakey-Milner, B. et al. (2021) ‘Metal additive manufacturing in aerospace: a review’, *Materials & Design*, Vol. 209, p.11000, https://doi.org/10.1016/j.matdes.2021.110008.

Cui, X. et al. (2006) 'Active polishing technology for large aperture aspherical mirror and ultra-thin mirror', *Proc. SPIE 6148, 2nd International Symposium on Advanced Optical Manufacturing and Testing Technologies: Large Mirrors and Telescopes*, p.614803.

Furuki, T. et al. (2014) 'Fabrication of magic-mirror with magnetic polishing and end-milling on machining center', *Transactions of the JSME*, in Japanese, Vol. 80, No. 820, p.DSM0390, https://doi.org/10.1299/transjsme.2014dsm0390.

Hibino, K. (1992) 'Mechanism of the production process of the Japanese magic mirror', *Applied Physics*, in Japanese, Vol. 61, No. 6, pp.600–603.

Hilpert, E. et al. (2018) 'Precision manufacturing of a lightweight mirror body made by selective laser melting', *Precision Engineering*, Vol. 53, pp.310–133.

Miller, S. et al. (1997) 'Fabrication of ultrathin mirrors for adaptive and space optics', *Proc. SPIE 3126, Adaptive Optics and Applications*.

Ni, Y. et al. (2006) 'Active support of ultra-thin mirror', *Proc. SPIE 6148, 2nd International Symposium on Advanced Optical Manufacturing and Testing Technologies: Large Mirrors and Telescopes*, p.61480X.

Pilseong, K. et al. (2017) 'New bending system using a segmented vacuum chuck for stressed mirror polishing of thin mirrors', *Current Optics and Photonics*, Vol. 1, No. 6, pp.618–625.

Romeo, R. et al. (2000) 'Ultralightweight and hyperthin rollable primary mirror for space telescopes', *Proc. SPIE 4013, UV, Optical, and IR Space Telescopes and Instruments*.

Roulet, M. et al. (2020) 'Use of 3D printing in astronomical mirror fabrication', *Proc. SPIE 11349, 3D Printed Optics and Additive Photonic Manufacturing II*, p.113490D.

Rousset, G. et al. (2003) 'NAOS, the first AO system of the VLT: on-sky performance', *Proc. SPIE 4839, Adaptive Optical System Technologies II*.

Saines, G. et al. (1999) 'Magic mirrors of the orient', *Journal of Optical Technology*, Vol. 66, No. 8, pp.758–765, https://doi.org/10.1364/JOT.66.000758.

Spiga, D. et al. (2016) 'Manufacturing an active X-ray mirror prototype in thin glass', *Journal of Synchrotron Radiation*, Vol. 23, Part 1, pp.59–66.

Susanto, A. et al. (2018) 'Milling process monitoring based on vibration analysis using Hilbert-Huang transform', *Int. J. of Automation Technology*, Vol. 12, No. 5, pp.688–698, https://doi.org/10.20965/ijat.2018.p0688.

Umezu, T. et al. (2019) 'Machining process for a thin-walled workpiece using on-machine measurement of the workpiece compliance', *Int. J. of Automation Technology*, Vol. 13, No. 5, pp.631–638, https://doi.org/10.20965/ijat.2019.p0631.

Yoneda, H. et al. (1978) 'Influence of the working process on the surface state and the reflection of the bronze mirror by casting', *Journal of the Faculty of Science and Technology, Kinki University*, in Japanese, Vol. 13, pp.185–194.

Zhang, H. et al. (2016) 'Study on machining deformation of the ultra-thin mirror', *Proc. SPIE 9683, 8th International Symposium on Advanced Optical Manufacturing and Testing Technologies: Advanced Optical Manufacturing Technologies*, p.968318.

Zhu, L. et al. (1999) 'Wave-front generation of Zernike polynomial modes with a micromachined membrane deformable mirror', *Applied Optics*, Vol. 38, No. 28, pp.6019–6026.